

# DESIGN AND COLD TEST OF A NOVEL WAVEGUIDE POWER SPLITTER FOR DISTRIBUTED POWER COUPLING IN SHORT-PULSE ACCELERATION

S. Colmekci\*, M. Shapiro, X. Lu<sup>1†</sup>

Northern Illinois University, DeKalb, IL, USA

<sup>1</sup>also at Argonne National Laboratory, Lemont, IL, USA

## Abstract

Radiofrequency (RF) breakdown is the major limitation to achieving higher accelerating gradients. Recent experimental evidence shows that this limitation can be mitigated by reducing the RF pulse length to a few nanoseconds at X-band frequencies. One key challenge in designing an accelerator operating in the short-pulse regime is achieving the required short filling time. In this work, we designed a novel waveguide power splitter that can be used to independently feed an array of accelerating cells. A prototype X-band waveguide array for a one-to-four power splitter has been designed, fabricated, and tested, where the input power is equally split into four output waveguides with the desired phase advance per cell. A 3D-printed prototype has been used for low-power microwave measurements. The results, including measurements in the frequency and time domains, agree well with the simulations. Ongoing work includes designing a multi-cell accelerator based on this concept for two-beam acceleration with short RF pulses.

## INTRODUCTION

A primary goal in designing radiofrequency (RF) accelerator structures is to enhance the accelerating gradient for a given input power while reducing the probability of RF breakdown. The likelihood of RF breakdown has been found to depend on both the accelerating gradient and the length of the RF pulse [1]. At a given breakdown rate, higher gradients can be achieved with shorter RF pulses. Recent studies have shown that short RF pulses on the order of a few nanoseconds can enable accelerating gradients approaching 300 MV/m [2, 3].

One challenge in designing an accelerating structure that operates with short RF pulses is achieving the required short filling time, particularly in a multi-cell structure. Distributed RF power coupling or individual power coupling [4–10] are promising concepts that could enable significantly shorter filling times. To operate cavities in this regime, an RF power distribution network is needed. This work presents a novel waveguide power splitter designed for distributed RF coupling in accelerator structures at X-band. Power splitting is achieved using specially designed septa on the shared waveguide walls.

A prototype of the power splitter has been designed, fabricated, and tested. In this one-to-four power splitter prototype,

the input RF power is equally divided among four parallel output waveguides at a center frequency of approximately 11.7 GHz, with a desired phase advance between adjacent output ports. The four output waveguides can be connected to individual accelerating cavities to drive them simultaneously and independently for short-pulse acceleration. This design can be adapted to waveguide systems at other frequencies.

## DESIGN AND SIMULATION OF THE WAVEGUIDE POWER SPLITTER

The X-band power splitter, operating with short RF pulses at 11.7 GHz, was designed using the computer simulation technology (CST) Microwave Studio. The frequency was selected based on the available wakefield power extractor at AWA, which provides short, high-peak-power RF pulses [2].

Figure 1 shows the vacuum model of the waveguide power splitter. It is designed to evenly distribute RF power among four output ports near the center frequency of 11.7 GHz and to provide a 90-degree phase advance between adjacent output ports. The design consists of one input port (Port 1 in Fig. 1), three identical septa, and four output ports (Ports 2–5 in Fig. 1). Each septum features a triangular-shaped cut on the shared broad waveguide wall to facilitate power splitting. The dimensions of the septa and waveguides can be tuned to adjust the phase and power distribution at the output ports. CST simulation results in both the frequency and time domains are presented in the next section and are benchmarked against the low-power measurement results.

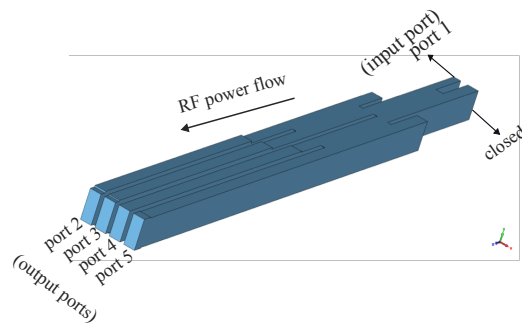


Figure 1: Vacuum part of the waveguide array power splitter, where power splitting is achieved by the septa design (not shown).

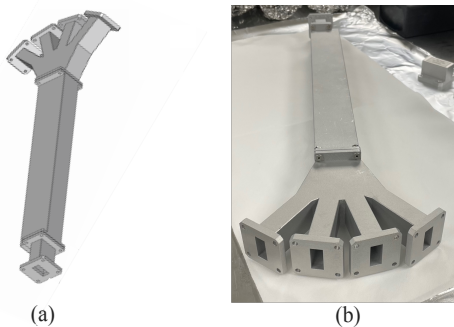


Figure 2: (a) Mechanical design version of the power splitter, including transitional pieces to facilitate the cold test. (b) 3D-printed waveguide array prototype.

## FABRICATION AND COLD TEST SETUP

Following the CST Microwave Studio simulations, we carried out the mechanical design of a prototype for low-power microwave measurements (i.e. cold test). Transitional pieces were added to the input and output ports, as shown in Fig. 2, to interface with standard WR90 waveguides at X-band for the cold test.

The model was divided into three sections, 3D-printed, and then assembled. Figure 2(a) shows the finalized mechanical design of the power splitter, including the transitional pieces for the cold test, and Fig. 2(b) shows the 3D-printed prototype, which was fabricated using the aluminum alloy AlSi10Mg to achieve a good surface finish.

Low-power microwave measurements were performed in both the frequency domain using a vector network analyzer (VNA) [see Fig. 3 (a)], and in the time domain using a signal generator to drive the input port and an oscilloscope to measure the output signals [see Fig. 3 (b)]. The signal generator was capable of producing short RF pulses with pulse lengths down to below 20 ns.

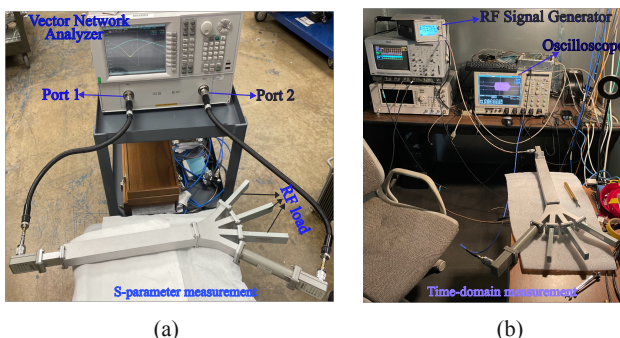


Figure 3: Experimental setups for (a) frequency-domain measurement using a vector network analyzer (VNA), and (b) time-domain measurement using a signal generator for the input signal and an oscilloscope for the output signals.

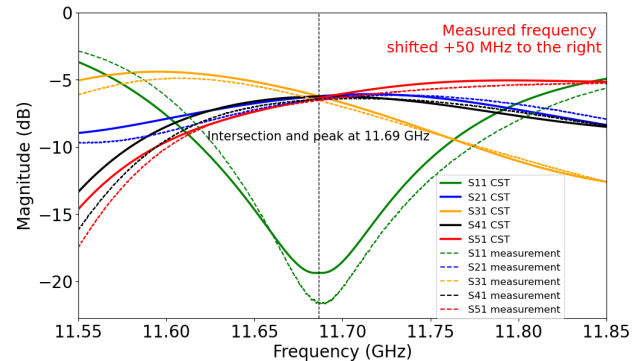


Figure 4: Simulated and measured magnitudes of the  $S$ -parameters ( $S_{21}$ ,  $S_{31}$ ,  $S_{41}$  and  $S_{51}$  for the four output ports, respectively) of the waveguide power splitter.

## COLD TEST RESULTS AND COMPARISON WITH SIMULATIONS

We measured the  $S$ -parameters during the frequency-domain cold test. The design goal was to transmit RF power from the input port to each output port with approximately 6 dB of insertion loss, while maintaining a  $90^\circ$  phase advance between adjacent output waveguides around the center frequency.

Table 1: Comparison of the Simulated and Measured  $S$ -Parameter Magnitudes at 11.69 GHz

| S-parameter magnitudes | Simulation dB | Measurement dB |
|------------------------|---------------|----------------|
| $ S_{11} $             | -19.31        | -21.49         |
| $ S_{21} $             | -6.19         | -6.46          |
| $ S_{31} $             | -6.26         | -6.54          |
| $ S_{41} $             | -6.23         | -6.47          |
| $ S_{51} $             | -6.25         | -6.55          |

Table 2: The Simulated and Measured Phase Advances Between Output Ports at 11.69 GHz

| RF phase diff. between ports | Simulation (degree) | Measurement (degree) |
|------------------------------|---------------------|----------------------|
| Port 2 and 3                 | 89.9                | 88.7                 |
| Port 3 and 4                 | 90.0                | 89.3                 |
| Port 4 and 5                 | 89.9                | 88.5                 |

Figure 4 shows both the simulated and measured  $S$ -parameter magnitudes, while Table 1 presents the detailed results at 11.69 GHz. An approximately uniform power distribution is achieved among the four output waveguides near the design frequency. The simulated and measured phase advances between output ports 2–3, 3–4, and 4–5 at 11.69 GHz are summarized in Table 2, indicating a  $90^\circ$  phase difference between adjacent output waveguides. The simulation and

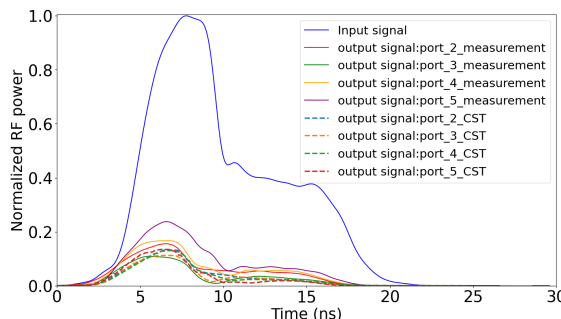


Figure 5: Time-domain measurements of the RF input power, where the input signal was generated using a signal generator. The measured output power at each port is benchmarked against simulation results. All the traces are normalized to the peak power of the input signal.

measurement results are in good agreement and confirm the intended functionality of the four-way power splitter.

Figure 5 shows the time-domain measurement results obtained using a signal generator and an oscilloscope. The input power waveform was used in CST time-domain simulations, and the resulting output port signals show good agreement with the measured waveforms. These results demonstrate that the prototype effectively performs power splitting in the short-pulse regime.

## FUTURE WORK

Design and optimization of a four-cell accelerating structure based on this waveguide power splitter are currently underway, as shown in Fig. 6. This approach can be extended to accommodate more than four output waveguides, and consequently, more accelerating cavities, while enabling tunable phase advances.

## CONCLUSION

This work presents a novel and compact RF power distribution technique based on a waveguide array, where power splitting is achieved using a septum design. Operating at X-band frequencies with short RF pulse durations, the waveguide power splitter enables efficient and uniform power delivery to a series of parallel waveguides, with controlled phase advances between adjacent cells. When used to drive

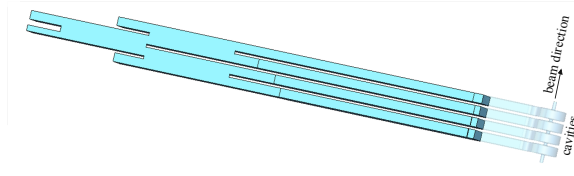


Figure 6: Future work aims to design a four-cell accelerating structure coupled to the parallel waveguide array power splitter.

an array of accelerating cavities, this configuration allows for short filling times by simultaneously feeding each cavity. A 3D-printed prototype was fabricated and tested using both frequency- and time-domain microwave measurements. The results show good agreement with simulations.

## ACKNOWLEDGMENTS

This research was supported by the U.S. Department of Energy, Office of Science, Office of High Energy Physics under Award DE-SC0021928.

## REFERENCES

- [1] A. Grudiev, S. Calatroni, and W. Wuensch, “New local field quantity describing the high gradient limit of accelerating structures”, *Phys. Rev. Spec. Top. Accel. Beams*, vol. 12, no. 10, 2009. doi:10.1103/physrevstab.12.102001
- [2] J. H. Shao *et al.*, “Generation of High Power Short Rf Pulses using an X-Band Metallic Power Extractor Driven by High Charge Multi-Bunch Train”, in *Proc. IPAC’19*, Melbourne, Australia, May 2019, pp. 734–737. doi:10.18429/JACoW-IPAC2019-MOPRB069
- [3] W.H. Tan, S. Liu, J. Shao, M. Peng, C. Jing, S. Antipov, C. Tang, “Demonstration of sub-GV/m accelerating field in a photoemission electron gun powered by nanosecond X-band radio-frequency pulses”, *Phys. Rev. Accel. Beams*, vol. 25, no. 8, p. 083402, 2002. doi:10.1103/PhysRevAccelBeams.25.083402
- [4] W. Gu *et al.*, “Design, fabrication, and test of a parallel-coupled slow-wave high-gradient structure for short input power pulses”, *Phys. Rev. Accel. Beams*, vol. 28, no. 6, p. 06041, 2025. doi:10.1103/dqpb-hst9
- [5] S. Tantawi, M. Nasr, Z. Li, C. Limborg, and P. Borchard, “Design and demonstration of a distributed-coupling linear accelerator structure”, *Phys. Rev. Accel. Beams*, vol. 23, no. 9, p. 092001, 2020. doi:10.1103/PhysRevAccelBeams.23.092001
- [6] Y. Jiang, J. Shi, H. Zha, J. Liu, X. Lin, and H. Chen, “Analysis and design of parallel-coupled high-gradient structure for ultrashort input power pulses”, *Phys. Rev. Accel. Beams*, vol. 24, no. 11, p. 112002, 2021. doi:10.1103/physrevaccelbeams.24.112002
- [7] W. Gu, H. Zha, H. Chen, J. Shi, and Q. Li, “Design of X-band distributed-coupling accelerating structure”, in *Proc. IPAC’24*, Nashville, TN, USA, May 2024, pp. 192–194. doi:10.18429/JACoW-IPAC2024-MOPC56
- [8] Z. Huang, Z. Cao, L. Sun, Y. Wei, and G. Feng, “Design of an X-band parallel-coupled accelerating structure for future linacs”, in *Proc. IPAC’24*, Nashville, TN, USA, May 2024, pp. 1454–1456. doi:10.18429/JACoW-IPAC2024-TUPR19
- [9] A. Dhar *et al.*, “Distributed Coupling Linac for Efficient Acceleration of High Charge Electron Bunches”, in *Proc. LINAC’22*, Liverpool, UK, Aug.-Sep. 2022, pp. 724–726. doi:10.18429/JACoW-LINAC2022-THPOJ014
- [10] X.Lu, Z. Li, V. Dolgashev, G. Bowden, A. Sy, S. Tantawi, and E. A. Nanni, “A proton beam energy modulator for rapid proton therapy”, *Rev. Sci. Instrum.*, vol. 92, no. 2, p. 024705, 2021. doi:10.1063/5.0035331